Quantum interference between two single photons emitted by independently trapped atoms

Jérôme Beugnon, Matthew P.A. Jones, Jos Dingjan, Benoît Darquié, Gaëtan Messin, Antoine Browaeys, Philippe Grangier

Quantum interference between two single photons emitted by independently trapped atoms

J. Beugnon[1], M. P. A. Jones[1], J. Dingjan[1], B. Darquié[1], G. Messin[1], A. Browaeys[1] & P. Grangier[1]

[1] *Laboratoire Charles Fabry de l'Institut d'Optique (UMR 8501),*

Bâtiment 503, Centre Universitaire, 91403 Orsay cedex, France .

When two indistinguishable single photons are fed into the two input ports of a beam splitter, the photons will coalesce and leave together from the same output port. This is a quantum interference effect, which occurs because the two possible paths where the photons leave in different output ports interfere destructively. This effect was first observed in parametric downconversion by Hong, Ou and Mandel [1], and then with single photons produced one after the other by the same quantum emitter [2–5]. With the recent development of quantum information, a lot of attention has been devoted to this coalescence effect as a resource for quantum data processing using linear optics techniques [6–11]. To ensure the scalability of schemes based on these ideas, it is crucial that indistinguishable photons are emitted by a collection of synchronized, but otherwise independent sources. In this paper, we demonstrate the quantum interference of two single photons emitted by two independently trapped single atoms, bridging the gap towards the simultaneous emission of many indistinguishable single photons by different emitters. Our data analysis shows that the coalescence observed is mostly limited by the wavefront matching of the light emitted by the two atoms, and to a lesser extent by the motion of each atom in its own trap.

A basic requirement for most quantum computing schemes is the implementation of two-qubit quantum gates [12]. If the qubits are encoded in single photons, the gate can be obtained by using an interference effect between the photons, followed by a measurement-induced state projection [6]. One may also use qubits encoded in solid-state systems such as quantum dots [13], or in atomic systems such as ions [14] or neutral atoms [15]. One way to entangle the atomic qubits without direct interaction, and thus realise quantum gates, is to use them as single photon sources, so that the emitted photons are entangled with the internal states of the emitters. The interference of two photons emitted by such sources projects the state of the two atoms into an entangled state [16]. Many protocols based on this conditional entanglement have been proposed [10,11], and experimental work is under way to implement them [17]. The photons involved in such schemes do not need to be initially entangled, and can even be emitted by different sources [9], but they need to be indistinguishable. However, it is generally not easy to have several (possibly many) independent sources emitting indistinguishable photons. With quantum dots in microcavities [2,3], the dispersion in frequency associated with differences in fabrication is usually much too large for the photons to be emitted at the same frequency. With atoms in cavities [4], each emitter is by itself a complicated experiment, and cannot be easily multiplied. In this paper we address this problem by using two single atoms in two neighbouring traps emitting in free space, and we demonstrate that these atoms do emit indistinguishable photons. This scheme can easily be scaled to arrays of traps [18].

Our experiment uses two single rubidium 87 atoms, confined in separate optical dipole traps. These traps are formed in the focal plane of the same high-numerical aperture lens, and loaded from a cloud of cold atoms in an optical molasses [19]. The two traps, each of which has a waist of 1 μm,

are separated by a distance of 6 μm. To obtain triggered single photon emission from the two atoms, we simultaneously excite them with a high efficiency ($> 95\%$) using a σ^+-polarised pulsed laser beam which drives the $F = 2,\ m_F = 2$ to $F' = 3,\ m'_F = 3$ closed transition [20]. The quantization axis is defined by a magnetic field of several gauss. Both atoms are excited by the same short (less than 4 ns) π-pulse. Each one then spontaneously emits a single photon [21], with a lifetime of 26 ns. The photons are collected by the same objective lens that is used to focus the dipole trap beams [19], and detected using a pair of avalanche photodiodes. Between the objective and the photodiodes, an optical setup composed of two half-wave plates and two polarizing beam splitter cubes (HWP1,2 and PBS1,2) is inserted in the beam path (see Figure 1). It can be configured either as a 50/50 beam splitter which mixes the light from the two atoms on each detector, or as a beam separator which sends the light from each atom to only one of the detectors. The avalanche photodiodes are connected to a high-resolution counting card in a start-stop configuration. This allows us to measure the number of coincident photodetections as a function of the delay between the arrival times of the two photons on the photodiodes, with a resolution of about 1.2 ns. In the 50/50 beam splitter configuration, the detectors cannot distinguish which atom has emitted a photon, and we expect to observe the coalescence effect. In the beam separator configuration, each avalanche photodiode only monitors the light emitted by one of the two atoms, and coincidence counts can only be due to independent emissions by both atoms.

The measurements are performed by repeating the following procedure. First, we detect the simultaneous presence of one atom in each trap in real time by measuring their fluorescence from the molasses light used to load the traps. We then trigger a sequence that alternates a burst of

575 pulsed excitations, lasting 115 μs, with a 885 μs cooling period using the molasses light. This alternation is repeated 15 times before stopping and recapturing a new pair of atoms. During the excitation periods, the π-pulses irradiate both atoms every 200 ns, and the counting card accumulates the number of double detections produced by the two avalanche photodiodes. This sequence maximizes the number of single photons that we can obtain before the two atoms are heated out of the trap [21]. After the 15 bursts of pulsed excitations, we measured a probability of 65% to keep each atom in its trap. At the end of the sequence, we switch the molasses back on and wait on average about 300 ms until we detect two atoms again. Two histograms are accumulated for the same number of repetitions: one in the 50/50 beam splitter configuration, and one in the beam separator configuration.

The two histograms are shown in Figure 2, without background subtraction. Both histograms consist of a series of peaks separated by 200 ns, the repetition period of the pulsed laser. The width of the peaks is determined by the 26 ns lifetime of the excited state. In the beam separator configuration, all peaks are identical, and always correspond to a double detection with one photon coming from each atom. Hence, their height gives a natural calibration of the experiment. A histogram in the 50/50 beam splitter configuration can be normalised by dividing by the height of the peaks in its corresponding histogram measured in the beam separator configuration. The normalized signals that are obtained are then independent of collection efficiency, detection efficiency and experiment duration, and allow histograms taken under different conditions to be compared. In the 50/50 beam splitter configuration, the peak at zero delay is clearly much smaller than the other peaks. As each atom is a very good source of single photons [21], this peak also consists only of events where both

atoms have emitted a photon. In contrast, the other peaks consist of events where two photons are successively emitted, either by the same atom, or by both atoms. Since the peaks at non-zero delay are almost the same in both configurations, we can deduce that almost all registered counts are due to events where both atoms were present.

In the case of perfect coalescence, the peak at zero delay in the 50/50 beam splitter configuration would be absent: as the two photons leave via the same port, there can be no coincidences. We attribute the residual peak that we observe in Figure 2 to an imperfect overlap of the spatial modes of the two photons, which then do not interfere. To experimentally illustrate this effect, we varied the overlap between the two modes in a controlled way by translating one beam relative to the other (translation of the cut mirror CM, see figure 1). Figure 3 shows the normalized height R of the residual peak at zero delay, as a function of the separation between the two images. For a given spatial overlap K between the amplitude of the two modes, the ratio R is expected to be $(1-K^2)/2$ (see Methods section). The solid line is a gaussian fit based on the experimental value of the beam size in the image plane, and considering the maximal wavefront overlap $K_{\max}$ as an ajustable parameter. The agreement with the coincidence data is very good, which confirms the crucial role of good mode matching of the two beams in our experiment. We obtain from the fit the maximum wavefront overlap $K_{\max} = 0.78 \pm 0.03$. This imperfect overlap is consistent with the errors we measure on the beam positions and waists.

Finally, we analyse the structure of the time spectrum around zero delay. The small peak at zero delay from Figure 2, is displayed on a larger scale in Figure 4. The dashed line correponds to

a model where the wavepackets of the two photons are identical and arrive at the same time on the beamsplitter, but with imperfect spatial overlap of the two beams. This curve does not correctly reproduce the experimental data: the experimental dots seem to sit on a slightly wider curve. Due to their finite temperature, the atoms move in the trapping potential and experience a range of light-shifts. This changes their internal energy, and thus modifies the frequency of the emitted photon. For two photons at different frequencies, the correlation signal would exhibit a beat note as already seen by Legero *et al.* [4]. If the two photons now have a distribution of frequencies, the correlation signal consists of a beat note averaged out over this distribution. This gives rise to a slightly broader structure for the signal, which is well fitted by the solid line predicted by our simple model (see details in the Methods section).

By fitting the experimental data shown in Figure 4 with our model, we extract the overlap of the spatial modes $K = 0.7 \pm 0.05$ and the temperature of the atoms $T = 180 \pm 20$ μK. In a separate experiment, we measured the temperature of the atoms in the dipole trap, which is initially close to 120 ± 10 μK. Each pulse followed by the spontaneous emission of the photon increases the energy of the atom by one recoil. We calculate that after the first 115 μsec of pulsed excitations the temperature rises by 60 μK, in good agreement with the temperature obtained from the fit above. We also checked experimentally that each cooling period resets the temperature of the atom to its initial value. A comparison of the fit with the dashed curve, which corresponds to zero temperature, confirms that at present the imperfect interference is mainly due to the imperfect optical wavefront matching, and not to the motion of the atoms in the traps.

In conclusion, we have experimentally demonstrated the coalescence of two photons emitted by two independent trapped atoms. The contrast of the interference is limited by the overlap (in free space) of the spatial modes of the fluorescence light emitted by the two atoms. By coupling the light from each of the atoms into identical single-mode optical fibres, this overlap could be greatly improved, though this may be at the cost of a reduced counting rate. The shape of the residual signal around zero delay is well explained by a broadening due to the finite temperature of the atoms in the trap. Better wavefront overlap and further cooling of the atoms will improve the overall quality of this interference and will make this system suitable as a resource for entangling two atoms.

Supplementary Information is linked to the online version of the paper at www.nature.com/nature.

Acknowledgements We acknowledge support from the European Union through the Integrated Project "SCALA". J. Dingjan was funded by Research Training Network "CONQUEST". M. Jones was supported by a Marie Curie fellowship.

Competing Interests The authors declare that they have no competing financial interests.

Correspondence Correspondence and requests for materials should be addressed to A. Browaeys (email: antoine.browaeys@iota.u-psud.fr).

Methods

Derivation of the experimental signal. If $f_k(\mathbf{r})\mathcal{E}_k(t)$ is the field emitted by the atom k ($k = 1, 2$), reference [22] shows that the probability to detect one photon at $\mathbf{r}_A$ and to detect the other one at $\mathbf{r}_B$, in the 50/50 beam splitter configuration, after a delay τ is proportional to

$$w^{(2)}(\tau, \mathbf{r}_A, \mathbf{r}_B) = \int |f_1(\mathbf{r}_B) f_2(\mathbf{r_A}) \mathcal{E}_1(t+\tau)\mathcal{E}_2(t) - f_2(\mathbf{r}_B) f_1(\mathbf{r}_A)\mathcal{E}_2(t+\tau)\mathcal{E}_1(t)|^2 \, dt,$$

which can be understood as the interference of two paths. Assuming a temporal form of the field $\mathcal{E}_k(t) = H(t)\, e^{-\frac{\Gamma}{2}t}\, e^{i\omega_k t}$ where $H(t)$ is the step function, we obtain

$$w^{(2)}(\tau) \propto e^{-\Gamma|\tau|}(1 - K^2 \cos\Delta\omega\, \tau),$$

where $K = |\int d\mathbf{r}\, f_1^*(\mathbf{r}) f_2(\mathbf{r})| / \sqrt{\int d\mathbf{r}\, |f_1(\mathbf{r})|^2 \times \int d\mathbf{r}\, |f_2(\mathbf{r})|^2}$ is the spatial overlap of the electric field, and $\Delta\omega$ is the frequency difference between the two emitted photons. The double detection probability for $\tau = 0$ is proportional to $(1 - K^2)$, and so is the normalised ratio R defined in the text. The proportionality factor is determined in the absence of interferences ($K = 0$): in this case, the two photons behave as distinguishable particles and have a probability of 1/2 to leave the 50/50 beam splitter through two different ports. Thus the normalised ratio R is $(1 - K^2)/2$.

Model including the finite temperature of the atoms in the trap. To take into account the finite temperature of the atoms in the trap, we integrate the expected signal for two photons interfering with a frequency difference $\Delta\omega$ and a spatial overlap K (see section above), over the probability distribution of frequency differences. To obtain this probability distribution, we solve the equations of motion for a thermal ensemble of single atoms in the trap, experiencing pulsed excitations during 115 μs, followed by a decay in a random direction. After each pulse, we calculate the lightshifts of

all the atoms in the ensemble. We repeat this for 575 pulses to obtain the distribution of lightshifts. This distribution is found to be well represented by a function of the form $U^2 e^{-\frac{2U}{k_B T}}$. The value of $\Delta\omega$ is proportional to the difference in lightshifts experienced by the atoms when they emit the photons. We then calculate the auto-correlation of the lightshift distribution to get the probability distribution of $\Delta\omega$. By averaging over this distribution of lightshift differences, we obtain the normalized coincidence rate signal as an analytical function with only two fitting parameters, the spatial overlap and the temperature of the atoms.

1. Hong, C. K., Ou, Z. Y., & Mandel, L. Measurement of subpicosecond time intervals between two photons by interference. *Phys. Rev. Lett.* **59**, 2044-2046 (1987).

2. Santori, C., Fattal, D., Vučković, J., Salomon, G. S., & Yamamoto, Y. Indistinguishable photons from a single-photon device. *Nature* **419**, 594-597 (2002).

3. Varoutsis, S., Laurent, S., Kramper, P., Lemaître, A., Sagnes, I., Robert-Philip, I., & Abram, I. Restoration of photon indistinguishability in the emission of a semiconductor quantum dot. *Phys. Rev. B* **72**, 041303(R) (2005).

4. Legero, T., Wilk, T., Hennrich, M., Rempe, G., & Kuhn, A. Quantum Beat of Two Single Photons. *Phys. Rev. Lett.* **93**, 070503 (2004).

5. Kiraz, A., Ehrl, M., Hellerer, Th., Müstecaplıoğlu, Ö. E., Bräuchle, C., & Zumbusch, A. Indistinguishable Photons from a Single Molecule. *Phys. Rev. Lett.* **94**, 223602 (2005).

6. Knill, E., Laflamme, R., & Milburn, G. J. A scheme for efficient quantum computation with linear optics. *Nature* **409**, 46-52 (2001).

7. Dowling, J. P., Franson, J. D., Lee, H., & Milburn, G. J. Towards Scalable Linear-Optical Quantum Computers. *Quantum Information Processing* **3**, 205-213 (2004).

8. Pan, J.-W., Bouwmeester, D., Weinfurter, H., & Zeilinger A. Experimental Entanglement Swapping: Entangling Photons That Never Interacted. *Phys. Rev. Lett.* **80**, 3891 (1998).

9. de Riedmatten, *et al.* Long-distance entanglement swapping with photons from separated sources. *Phys. Rev. A* **71**, 050302 (2005).

10. Lim, Y. L., Beige, A. & Kwek, L. C. Repeat-Until-Success Linear Optics Distributed Quantum Computing. *Phys. Rev. Lett.* **95**, 030505 (2005).

11. Barrett, S. D., & Kok, P. Efficient high-fidelity quantum computation using matter qubits and linear optics. *Phys. Rev. A* **71**, 060310 (2003).

12. Zoller, P., Cirac, J.I., Duan, L., & García-Ripoll, J. J. Quantum optical implementation of quantum information processing. *Les Houches, Session LXXIX, 2003 - Quantum entanglement and information processing* (eds. Estève, D., Raimond, J.-M., & Dalibard, J.) 187-222 (Elsevier, Amsterdam, 2004).

13. Paillard, M., Marie, X., Renucci, P., Amand, T., Jbeli, A., & Gérard, J.-M. Spin Relaxation Quenching in Semiconductor Quantum Dots. *Phys. Rev. Lett.* **86**, 1634-1637 (2001).

14. Monroe, C., Meekhof, D. M., King, B. E., Itano, W. M., & Wineland, D. J. Demonstration of a Fundamental Quantum Logic Gate. *Phys. Rev. Lett.* **75**, 4714-4717 (1995).

15. Schrader, D., Dotsenko, I., Khudaverdyan, M., Miroshnychenko, Y., Rauschenbeutel, A., & Meschede, D. Neutral Atom Quantum Register. *Phys. Rev. Lett.* **93**, 150501 (2004).

16. Simon, C., & Irvine, W. T. M. Robust Long-Distance Entanglement and a Loophole-Free Bell Test with Ions and Photons. *Phys. Rev. Lett.* **91**, 110405 (2003).

17. Blinov, B. B., Moehring, D. L., Duan, L.-M., & Monroe, C. Observation of entanglement between a single trapped atom and a single photon. *Nature* **428**, 153-157 (2004).

18. Bergamini, S., *et al.* Holographic generation of microtrap arrays for single atoms by use of a programmable phase modulator. *J. Opt. Soc. Am. B* **21** 1889-1894, (2004).

19. Schlosser, N., Reymond, G., Protsenko, I., & Grangier, P. Sub-poissonian loading of single atoms in a microscopic dipole trap. *Nature* **411**, 1024-1027 (2001).

20. Dingjan, J. , Darquié, B. , Beugnon, J. , Jones, M.P.A, Bergamini, S. , Messin, G., Browaeys, A., & Grangier, P. A frequency-doubled, pulsed laser system for rubidium manipulation *Appl. Phys. B* **82**, 47-51 (2006).

21. Darquié, B., *et al.* Controlled Single-Photon Emission from a Single Trapped Two-Level Atom. *Science* **309**, 454-456 (2005).

22. Legero, T., Wilk, T., Kuhn, A., & Rempe, G. Time-resolved two-photon quantum interference. *Appl. Phys. B* **77**, 797-802 (2003).

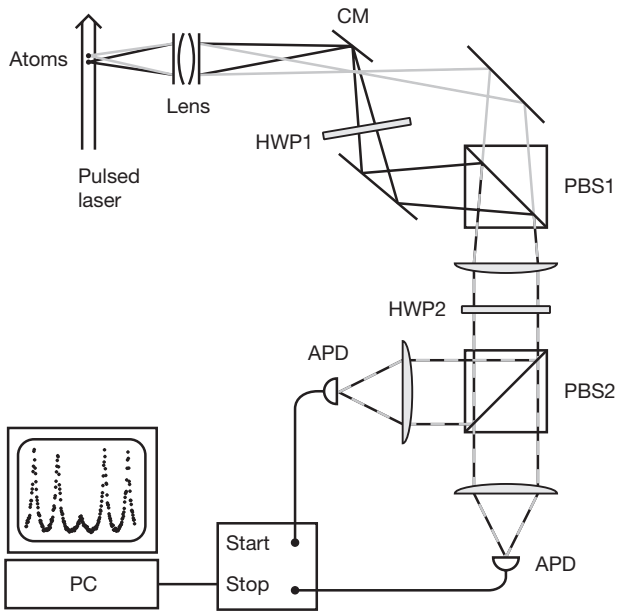

Figure 1: Experimental setup. The two atoms are trapped in two dipole traps separated by 6 μm, and they are excited by the same pulsed laser beam. The trap depth is 1.5 mK, and the trap frequency along the axis of the pulsed laser beam is 120 kHz. The emitted photons are collected by the same lens that is used to create the dipole traps. The light from one of the traps is separated off using a cut mirror (CM) placed close to the image plane of the objective. In the plane of the cut mirror, the spot corresponding to each trap has a waist of ~ 90 μm, and the two images are separated by 500 μm. The half wave plate HWP1 is oriented such that, at PBS1, the light beams from the two atoms are recombined into the same spatial mode, but with orthogonal polarizations. There are then two configurations to detect the photons: either the axis of the half-wave plate HWP2 is set so that the two orthogonal incident polarisations are equally mixed in each output of PBS2, as in a 50/50 beam splitter, or the axis is set so that the polarisations are unchanged, and then PBS2 simply separate the two beams coming from the two atoms without mixing them. Two avalanche

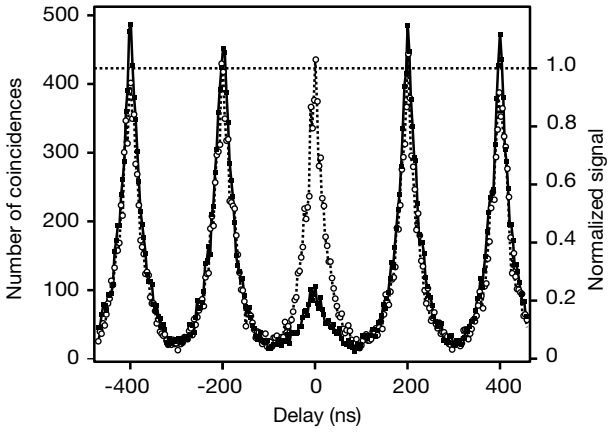

Figure 2: Histograms of the time delays of the arrival of two photons on the avalanche photodiodes, in the start-stop configuration. Black squares correspond to the 50/50 beam splitter configuration (interfering beams). Empty circles correspond to the beam separator configuration (independent beams). These histograms have been binned 3 times leading to a 3.6 ns resolution. The total accumulation time is about 5 hours, corresponding to about 6600 events with two photons arriving on the beam splitter around zero delay. The solid and dashed lines are a guide to the eye. The normalized signal is obtained by dividing the number of counts by the average value of the peak height in the beam separator configuration.

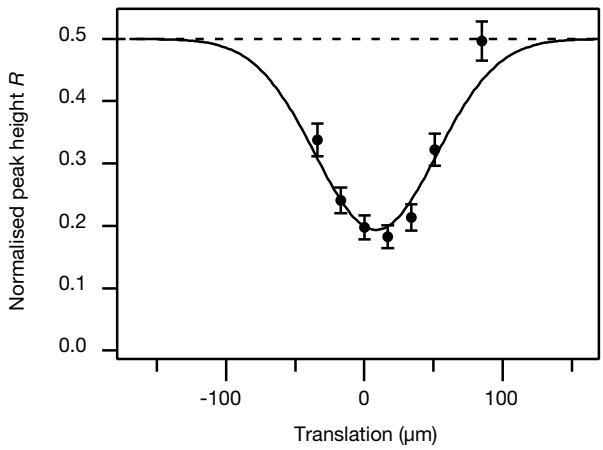

Figure 3: Ratio of the height of the residual peak at zero delay in the beamsplitter configuration to the average height of the peaks in the beam separator configuration, as a function of the relative distance between the two beams, translated parallel to each other. The solid curve is the expected ratio, calculated from the measured beam waist of the two beams. The amplitude and the center of this curve is adjusted to fit the data. The error bars correspond to statistical uncertainties.

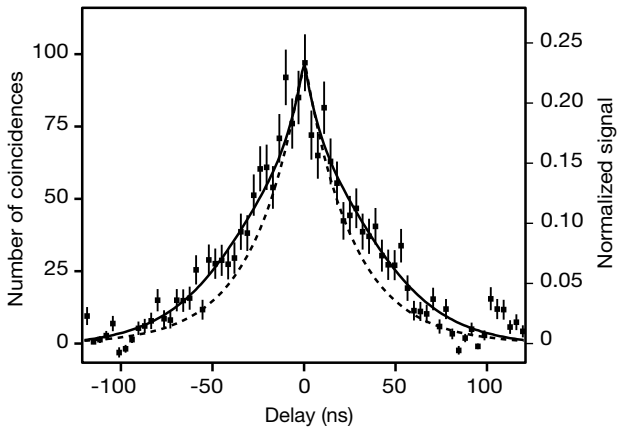

Figure 4: Zoom of the histogram of Figure 2 in the 50/50 beam splitter configuration, around zero delay. This curve is obtained from Figure 2 by subtraction of the contribution from the background and neighbouring peaks. The squares represent the experimental data expressed in number of coincidences. The solid line is a fit by the model described in the Methods section, taking into account the finite temperature of the atoms and the spatial overlap. The dotted line is the expected signal for zero temperature. The error bars correspond to statistical photon counting noise.

Supplementary Material

The following appears as Supplementary Online Material in the published version.

A: THE NORMALIZED HEIGHT OF THE RESIDUAL PEAK FOR NON-INTERFERING PHOTONS

In the absence of interference, i.e. if the spatial overlap $K = 0$, the height of the peak at zero delay after the normalization described in the text is 0.5. The reason why it is 0.5 and not 1 can be understood from the following argument. The normalised peak height, as described in the text, is simply the height of the peak in the beam splitter configuration divided by the height of the peak in the beam separator configuration, both taken at zero delay. At zero delay, a coincidence event, whether in the beam splitter or beam separator configuration, always corresponds to the detection of one photon from each atom. This is because both atoms are near perfect single photon sources, and therefore the probability that one of the atoms emits two photons during the same excitation/emission cycle, which would appears as a peak et zero delay, is negligible.

The difference between the two configurations is that in the beam separator configuration, where each photodiode sees the light from only one of the atoms, a pair of photons where one photon comes from each atom always gives rise to a coincidence. In the beam splitter configuration, both of the photons can end up at the same photodiode, as each photodiode sees both atoms. In this case, no coincidence occurs. For a 50-50 beamsplitter and distinguishable, non-interfering photons, this happens 50% of the time. The same number of incident photon pairs therefore gives

rise to half as many concidences in this configuration and thus the ratio of the heights of the peak at zero delay in the two configurations is 0.5.

B: ALIGNMENT OF THE OPTICAL SYSTEM AND LIMITS ON SPATIAL OVERLAP.

In order to overlap the spatial modes of the two single photons in free space, we used the fluorescence signal of each of the two single atoms induced by the magneto-optical trap laser beams. We measured the beam positions and waist ($1/e^2$ radius) in two perpendicular directions and at two positions along the propagation axis by taking intensity profiles using razor blades. Using such profiles, the angular and translational alignment were corrected step-by-step. This process was ultimately limited by the error bars introduced by intensity fluctuations on the single atom signal. The translational alignment (x and y) of the two spatial modes was further improved using the contrast of the two-photon interference signal itself, as shown in figure 4.

To understand how possible alignment errors contribute to the spatial overlap, we have estimated how much the overlap changes in the following situations:

1. The two beams have a different waist (different divergence).

2. The two beams are displaced transversally (x and y).

3. The position of the focal plane along the optical axis is different for the two beams.

4. The two propagation axes have a small angle between them.

In order to get an electric field mode overlap $K > 0.8$, one should achieve better than a 4% error on each of these alignements, assuming that they are independent. As an example, if the size of the waist of the two beams is different by 16%, which corresponds to our error bar on the waist size, then the overlap K is already multiplied by 0.97. The cumulative effect of small alignment errors seems therefore a reasonable explanation for the limited spatial overlap that we observe. However, it should be noted that phase errors across the wavefronts of the two beams due to aberrations of the optical system would also decrease the spatial overlap.

C: THE EFFECT OF INHOMOGENEOUS BROADENING ON THE SHAPE OF THE RESIDUAL PEAK AT ZERO DELAY

The finite temperature of the atoms in the dipole traps gives rise to an inhomogeneous broadening of the spectrum of the photons emitted by the atoms. As described in our article, this broadening manifests itself in our two-photon interference signal as an increase in the width of the residual peak at zero delay. The height of the residual peak, is not changed, and depends only on the spatial overlap of the two beams.

In the case of perfect spatial overlap, the peak would disappear at exactly zero delay. This is because if one looks close enough around zero delay, the wavepackets of the two photons look alike as dephasing due to their frequency difference has not had time to occur. In a sense, perfect two-photon interference always occurs, provided we look at "short enough" timescales. This is equivalent to imposing temporal coherence by adding a narrow band filter. In the case of perfect

spatial overlap, our residual peak would have a “dip” at exactly zero delay, with the width of this dip depending on the inhomogeneous spectral width of the emitted photons. This effect has been observed for two photons emitted by the same source [4], and the theory is detailled in ref [22]. The figure below summarizes this different configurations.

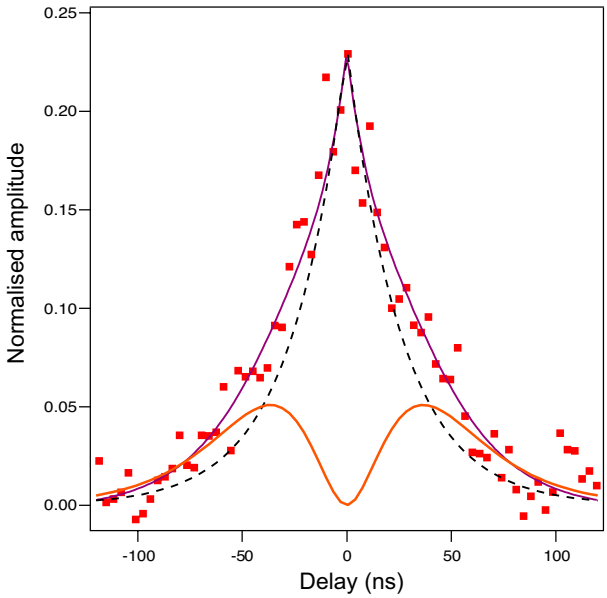

Figure 5: Zoom of the histogram of Figure 2 in the 50/50 beam splitter configuration, around zero delay. This curve is obtained from Figure 2 by subtraction of the contribution from the background and neighbouring peaks. The squares represent the experimental data expressed in number of coincidences. The solid line is a fit by the model described in the Methods section, taking into account the finite temperature of the atoms and the spatial overlap. The dotted line is the expected signal for zero temperature. The solid line with a dip at zero delay is the expected signal for a perfect spatial overlap and a temperature of 200 μK. This shows that at zero delay, in the case of a perfect spatial overlap, the interference is always perfect, whatever the temperature is.